TECHNICAL UNIVERSITY OF CLUJ-NAPOCA

ACTA TECHNICA NAPOCENSIS

Series: Applied Mathematics, Mechanics, and Engineering
Vol. 67, Issue Special I, February, 2024

POLYETHERETHERKETONE (PEEK) IN RAPID TOOLING: ADVANCEMENTS AND APPLICATIONS FOR FUSED FILAMENT FABRICATION OF RUBBER MOLDS

Karim ABBAS, Nicolae BALC, Sebastian BREMEN, Lukas HEDWIG

Abstract: *Establishing high-performance polymers in additive manufacturing opens up new industrial applications. Polyetheretherketone (PEEK) was initially used in aerospace but is now widely applied in automotive, electronics, and medical industries. This study focuses on developing applications using PEEK and Fused Filament Fabrication for cost-efficient vulcanization injection mold production. A proof of concept confirms PEEK's suitability for AM mold making, withstanding vulcanization conditions. Printing PEEK above its glass transition temperature of 145 °C is preferable due to its narrow process window. A new process strategy at room temperature is discussed, with micrographs showing improved inter-layer bonding at 410°C nozzle temperature and 0.1 mm layer thickness. Minimizing the layer thickness from 0.15 mm to 0.1 mm improves tensile strength by 16%.*

Keywords: *Additive Manufacturing; Fused Filament Fabrication; Tensile Strength; Polyetheretherketone (PEEK); Rapid Tooling; Process Parameters*

1. INTRODUCTION

Additive Manufacturing, also known as 3D printing, has emerged as a transformative technology that is revolutionizing various industries worldwide. Unlike traditional subtractive manufacturing methods, where the material is removed to obtain the desired shape, additive manufacturing builds objects layer by layer, offering unparalleled design freedom and manufacturing efficiency. A number of manufacturing processes using metal- and polymer-based materials have been established in the industry. Metal additive manufacturing has found diverse applications in aerospace, automotive, healthcare, and other industries, enabling the production of customized, high-performance components with superior mechanical properties [1]. The applications of polymer additive manufacturing are wide and include all kinds of industries. Components can be produced quickly with low cost and low quantities. Limitations are the low melting point of the thermoplastic materials and lower strength and stiffness when compared to metal materials. Polymer AM processes can be divided into technologies based on photopolymerization, material extrusion, material jetting, and powder bed processes, among others [1, 2].

This research work focuses on the so-called Fused Filament Fabrication (FFF for short), one of the most well-known and commercial AM processes [3]. FFF is a material extrusion process based on the temporary melting of thermoplastic polymers. It was developed in the 1990s by the Stratasys company and enabled the production of complex geometries. FFF is also known as Fused Deposition Modelling (process name of the Stratasys company) [4].

The FFF process is a strand deposition process that heats a thermoplastic polymer above the glass transition temperature using a heated print head or heated nozzle and applies it layer by layer [5]. The starting materials are usually in wire form. The material is applied to a, usually heated, plate and fixed to it by an adhesion promoter or existing adhesion mechanisms. The material is pressed through the circular outlet of the nozzle by an extruder and then applied in a geometrically defined manner.

The distance between the nozzle and the underlying substrate or layer is usually smaller than the nozzle diameter. This gives the deposited strand a geometrically defined shape. The cross-section corresponds to an ellipse. The chosen layer height ensures the connection of the new and old layers. The layered material solidifies after application through heat conduction processes. The build-up direction is in the direction of the Z-axis for most FFF systems, and the layers are placed in the XY plane. Due to the material placement in the XY plane, FFF is in the broadest sense, a 2½ dimensional process and not a 3D process. However, new research approaches in non-planar printing pursue a new strategy by adding the Z-axis [6].

A wide range of process materials can be used, from simple polymers, technical polymers, and filled polymers to high-performance and fibre-reinforced polymers, which can also be processed with consumer-friendly desktop FFF systems. The wide range of materials and the increasingly better systems enable the FFF to be used in both rapid manufacturing and rapid prototyping. [7]

Manufacturing injection molds is a complex process consisting of many iterative processes and development steps that are very time- and cost-intensive. Due to ever-shorter product life cycles and new product variants, the time and cost pressure on the production of injection molds is increasing. Conventional manufacturing processes quickly reach their limits, which creates the need for efficient and economical solutions. [8, 9]

High-performance polymers offer future-oriented potential in the field of injection mold production. In particular, the advantages of the polymers can be exploited and utilized through the current possibilities of additive manufacturing.

Polyetheretherketon (PEEK) has already established itself as a high-performance polymer in various sectors, such as the automotive industry or medical technology [10]. In AM, too, there are more and more approaches for improved material processing using FFF and Selective Laser Sintering. Still, no generally valid guideline allows users to process the material reliably and reproducibly.

PEEK is a semi-crystalline thermoplastic with a very high melting temperature of 343 °C compared to other thermoplastics [11]. The excellent mechanical properties, high biocompatibility, and chemical resistance make PEEK an interesting material for many application areas [11]. Components made of PEEK are used, in electrical engineering as insulation, in medical technology as parts of surgical instruments or as short-term implants, and in mechanical engineering as gearwheels, bushings, or pump parts [12]. Manufacturers state the tensile strength to be up to 100 MPa the compressive strength up to 125 MPa [10].

Rapid Tooling is supposed to increase economic efficiency, shorten the development process, and increase flexibility in production. The Swiss company LIM Technics OOD, focusing on injection molding, investigated the economic efficiency and the associated time savings using PEEK molds in a case study. The entire manufacturing process, from design to the finished tool, as compared to a standard mold, considering the time and costs involved.

Based on the tested demonstrator, the study showed that production costs could be reduced by up to 86% in both low-wage and high-wage countries. The time saving was 66% and was reduced from 6 to 2 days of development and production [13].

Dizon et al. [14] and the researchers Parkt et al. investigated PEEK in the context of Rapid Tooling. The entire manufacturing process was investigated during the research work, from developing a suitable extruder to the necessary process parameters. Three demonstrators, including an injection mold, were made of PEEK and tested for different applications. The injection molding tool lasted 112 shots without any further signs of wear.

The ring elements made of polypropylene produced with this tool had a deviation of only 0.07%-0.25% in dimensional accuracy. This test demonstrated the dimensional stability of the tool. The mechanical parameters, such as tensile strength, reached up to 90 % of conventionally produced samples. However, it is unclear from the tests which printing strategy was finally used for the tool [15].

All of the previously mentioned areas of application of rapid tooling in the field of

polymer AM deal preferentially with the classic injection molding process of thermoplastics. In the cases mentioned, the mold temperatures were below the glass transition temperature of the mold materials. However, the decisive load case for vulcanization is in the high-temperature range of up to 200 °C. A first pilot study on this has already been conducted by Vassallo et al. [16], which, to the author's knowledge, is the only study on using PEEK as a tooling material for elastomers. In the study by Vassallo et al., rubber components were manufactured at 182°C in FFF manufactured PEEK molds.

Currently, research is limited to the additive manufacturing of PEEK in a heated build chamber. In this way, the PEEK component is completely crystallized, and an improved layer bonding should be achieved. However, complex temperature management often leads to stress-induced crystallization and, thus, to process errors and process failures.

The still little-established PEEK FFF Printers pursue process strategies with build chamber temperatures (BCT) below and above the glass transition temperature of approx. 145 °C [17–19].

This work aims to investigate a new FFF process strategy of PEEK at room temperature and validate the main process variables.

Using the developed FFF process parameters, an injection mold for vulcanization is manufactured, and its durability is investigated.

2. MATERIALS AND METHODS

Initially, different nozzle temperatures (390°C - 430°C) above the melting temperature and layer thicknesses (0,1-0,15 mm) are tested. The FFF process takes place at room temperature with an open build chamber. Hollow cubes with three different wall thicknesses are printed, then embedded, ground, and polished up to 3 µm grit size. By varying the wall thickness, thermal insulation effects are to be revealed since the cooling rate and layer bonding are influenced by the layers in contact. At the same time, the connection to the lower and adjacent layers is broken down. Accordingly, the sample section is to reveal the quality of the bonding. In order to evaluate the influence on the mechanical properties, additional tensile tests are carried out.

2.1 Tensile test and optical analysis

The tensile test was performed using a Zwick Roell 10 kN tensile machine. In accordance with DIN EN ISO 527-1, bone-shaped specimens of type 1.BA were printed. The samples were printed at room temperature using a custom designed system. The specimens were printed horizontally and with an infill density of 100%. The layer thickness was 0.1 mm and 0.15 mm. The printing speed was 40 mm/s. A preload of 1 MPa was selected and a test speed of 50 mm/min. At least three samples of the material were tested after FFF and after thermal post-treatment. To clarify the influence of the BCT and a thermal post-treatment, additional comparison samples were FFF-manufactured at a build chamber temperature of 150 °C and a layer thickness of 0.1 mm.

Subsequently, the fracture surfaces were examined using a Sigme 300 – Feldmissions scanning electron microscope (SEM) The images are a secondary electron (SE) image generated with an accelerating voltage of 15 KV and a working distance (WD) of 7.1 mm. Additional micrographs were taken using a digital Keyence VHX 1000 microscope.

2.2 Rapid tooling and vulcanization molding

Based on the developed process parameters, a three-part injection mold consisting of two mold halves and a core was manufactured using FFF and PEEK. The FFF process took place at room temperature, a nozzle temperature of 200°C, and a layer height of 0.1 mm. The filament is the "ThermaX™ PEEK" from the company “3DXTech Additive Manufacturing”.

A 3DGence laboratory furnace was employed to carry out the thermal post-treatment of the mold. The mold was gradually heated to reach the designated temperature of 250 °C over a span of 11 hours, utilizing precise temperature control. Following this, the moldparts were maintained at this temperature for a duration 5 hours respectively. Subsequently, a controlled cooling process spanning 15 hours was employed to gradually bring the samples back to room temperature. This gradual cooling

approach was adopted to ensure consistent cooling rates across the specimens, minimizing the risk of stress induction that might result from rapid cooling.

The PEEK injection mold was heated to 200°C in a master mold and then filled with an Ethylen-Propylen-Dien-(Monomer) rubber using a manual laboratory press. The rubber component was vulcanized for approx. 12min.

3. RESULTS AND DISCUSSION

3.1 Micrographs

The following Fig. ***1*** shows the micrographs of the specimens with just one wall. The quality differences, as well as induced defects, are clearly visible here. The two different layer thicknesses, 0.15 mm, and 0.1 mm, already show considerable and significant differences between the process strategies.

First and foremost, it can be seen that in all 0.15 mm samples, the expression and number of pores are increased. In addition, the deposited strands show an uneven shape and, in some cases, missing bonds. This contrasts with the 0.1 mm specimens, whose expression is homogeneous and uniform. On the other hand, the thermally post-treated specimens show only minor differences compared to the non-treated specimens.

Apart from the layer height, the nozzle temperature significantly influences the samples and layers. In particular, the specimens printed at 390 °C with a layer height of 0.15 mm have a heterogeneous appearance of the strands. The strand widths vary considerably here between 223-430 µm. This leads to samples with additional walls not being connected to the adjacent strands. Accordingly, large cavities are found between adjacent walls (Fig. ***2***).

There are pores within the deposited strands and in the boundary layers of the strands. In all cases, the most prominent pores with a diameter of up to 102 µm are located within the strand. In contrast, the boundary layer pores are distributed over the entire boundary layer region and are over ten times smaller. With the temperature increase to 410°C, the print image improves immensely. The subsequent temperature increase to 430°C shows a decline in the quality of the samples. Again, there are pores with sizes up to 100 µm within the strands, and additional boundary layer pores up to 45 µm in diameter. Nevertheless, the strand width remains uniform throughout.

The best results, in terms of optical analysis, have been determined at 0.1 mm layer height. The weld and strand pattern improved at all three nozzle temperatures. All specimens of the measuring series with 0.1 mm layer height show a reduction of pore formation. In particular, the samples printed at 390°C and 430°C have only small boundary layer pores and isolated tiny pores within the strands.

The layer height and width are similar in all cases and show only minimal deviations from each other and the nominal dimension. This is especially true for the test series printed at 390°C and 410°C nozzle temperatures. The test series printed at 430°C shows fluctuations in the layer width, resulting in minimal inhomogeneity in the printed image.

During the examination of the samples, it is first noticed that all specimens have an opaque colour. After thermal post-treatment in the oven, the sample colour changes and turns beige.

3.2 Discussion on the nozzle temperature

The present study on the nozzle temperature provides the first significant insights into the additive manufacturing of PEEK at room temperature. By the untreated samples' colour, it can be concluded that the material is in an amorphous state. Subsequent thermal post-treatment changes the material colour to opaque and indicates the crystallized phase. At first glance, all samples show no defect in their outer form.

Only the micrographs reveal the considerable differences and the effects of the process strategies. First and foremost, the study indicates that the print image becomes more homogeneous and uniform with increasing nozzle temperature. A closer look reveals that the most extensive defects are the deposited strands' pores and reduced transition zones.

These defects can be attributed to the following causes, among others [20]: Relative velocity from the nozzle to print bed - Shear rate; Viscosity; Moisture of the filament; Feeding of air through the nozzle; Crystallization behaviour.

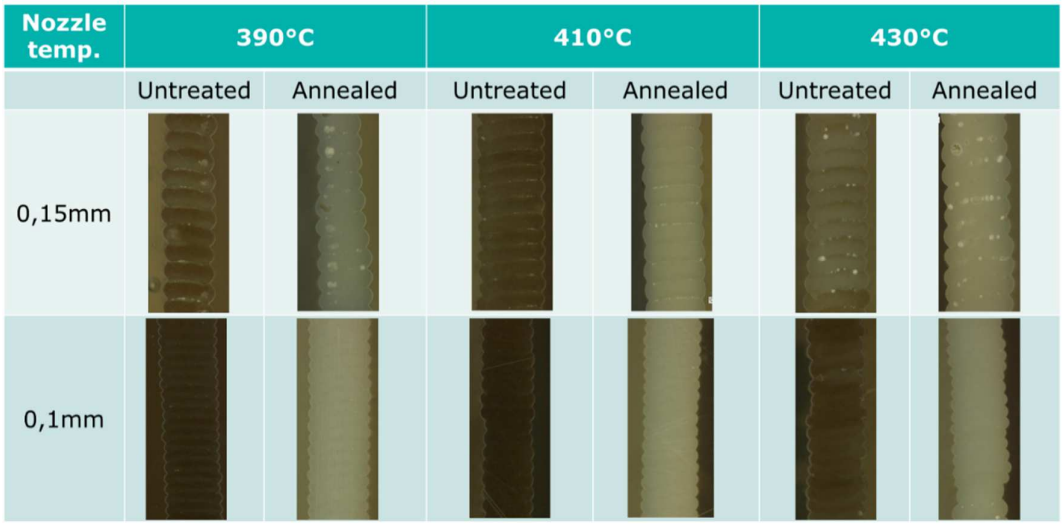

Fig. 1 Micrographs of PEEK specimens (one wall thickness)

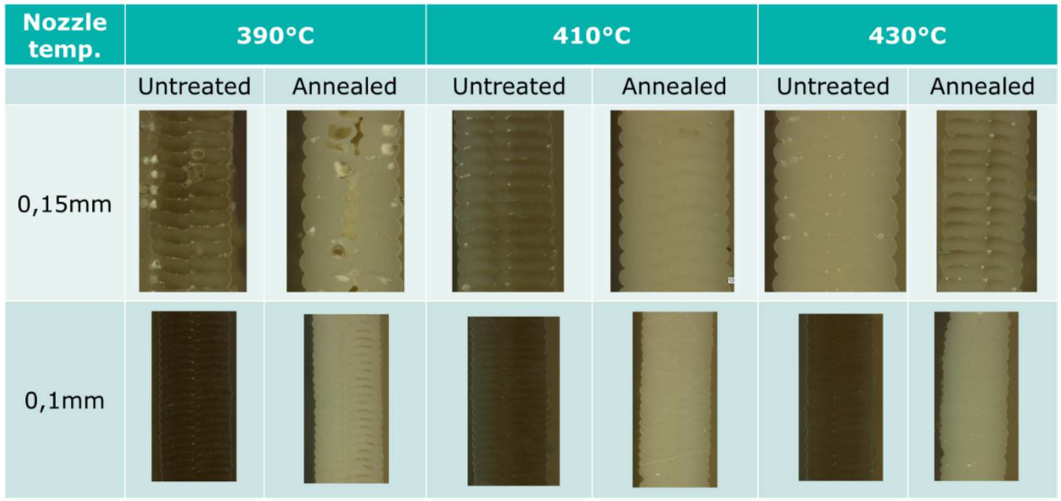

Fig. 2 Micrographs of PEEK specimens (two wall thicknesses)

Right at the beginning, several of these assumptions can be refuted. The quality of the filament is very high, and the diameter deviations are in the range of +/- 0.05 mm, so it can be ruled out that these are quality defects of the filament. Since PEEK can exhibit slight hydrophilicity, pores may form during extrusion. Water trapped in the polymer evaporates within the melt, expanding and providing cavities. Since the filament was dried in an oven at 200°C before each use, this influencing factor can also be excluded.

The layer thickness and the nozzle temperature provide the essential indications and influencing variables. The pores are reduced by reducing the layer thickness to 0.1 mm and increasing the nozzle temperature to 410-430°C. This fact leads to the assumption that primarily the material's viscosity and the solidification behaviour of PEEK are responsible for the pore formation. The material appears to have a too high viscosity at 390 °C, which prevents the deposited strands from forming a uniform structure and interlayer bonding. This leads to misshapen strand cross-sections that simultaneously indicate insufficient wettability. According to [21, 22], the nozzle temperature must be above the crystallization temperature for successful interlayer bonding of semi-crystalline polymers.

The crystallization temperature of the PEEK tested here is approx. 301 °C. Accordingly, the melting temperature of 390 °C should already be sufficient to cause a corresponding neck growth.

However, neck growth competes with crystal formation and material cooling simultaneously.

In this context, it should not be neglected that the FFF process is carried out at room temperature, and the material solidifies amorphously. The consequence of the low ambient temperature, the comparatively large layer thickness, and the heat conduction process most likely lead to a rapid viscosity increase. The high viscosity results in trapped voids that cannot escape from the melt track.

It is only by increasing the nozzle temperature that the melt viscosity is decreased, and void formation reduced. Since the samples crystallize amorphously even at high nozzle temperatures, it can be assumed that the cooling rates are so high that crystallization is prevented. It is unclear why enlarged pores form in the boundary layers despite the increased nozzle temperature of 430°C. Vaezi et al. also found pores as well as color differences in samples printed above 430°C, indicating degradation [23]. One assumption is that the increased nozzle temperature causes the formation of pores in the boundary layers. One hypothesis is that the high temperature causes the degradation of additives, whose degradation products escape during the process.

The layer thickness reduction carried out in the next step provides further information on the relationship between the nozzle temperature and interlayer bonding. For all samples, the reduction to 0.1 mm layers significantly minimizes the pore formation and improves neck growth and, thus, interlayer adhesion. Similar results are obtained by researchers [24, 25].

It is assumed that the decrease in the layer thickness counteracts the rapid increase in viscosity. In addition, the reduction improves the escape of trapped air. With the layer thickness reduction, the nozzle's heat influence area can also positively influence the strand deposition. In addition, the heat flux of the nozzle is higher for small layer thicknesses than for large layer thicknesses [26].

A simplified one-dimensional view of the heat flow, using steady-state heat conduction, would be higher for small layer thicknesses than for large layer thicknesses. This would support the assumption that the approach of the nozzle to the previously deposited layer has a positive effect on the inter-layer bonding. First, time is primarily neglected as a factor. The adjacent nozzle (nozzle temperature T_N) and the base layer (layer temperature T_L) on which a new strand is deposited now provide a temperature gradient. The deposited strand (layer thickness s) represents a thermal resistance R_λ for which applies (1) [27]:

$$R_\lambda = \frac{\Delta T}{\dot{Q}} = \frac{s}{\lambda \cdot A} \qquad (1)$$

This results in the following for the heat flow (2):

$$\dot{Q} = \frac{\lambda \cdot A \cdot (T_N - T_L)}{s} \qquad (2)$$

Consequently, the reduction of the layer thickness increases the heat flux. Thus, a positive influence by the nozzle can be assumed.

3.3 Results and discussion on the tensile strength

Table 1 compares the average tensile strengths of the specimens. Several results crystallize here. Starting with the layer thickness, it can be seen that specimens with a layer thickness of 0.1 mm have tensile strengths almost 10 MPa higher than the 0.15 mm layer. Thermal post-treatment even increases the tensile strength by up to 10 MPa. The tendency for 0.1 mm layers to have higher tensile strengths remains even after thermal post-treatment. At 0.1 mm layer thicknesses, tensile strengths of 73.8 MPa are achieved. In comparison, in situ crystallized tensile specimens additively manufactured at a BCT of 150°C reached only 70 MPa.

Table 1

Comparison of the tensile strength

Layer Height	Tensile Strength [MPa]		Elongation at beak [%]	
	Untreated	Annealed	Untreated	Annealed
0,15mm	56,7	63,2	10,6	11,2
0,1mm	63,4	73,8	9,2	9,4
In-Situ Crystallized				
0,1mm	70		11,4	

Additional SEM images were taken to interpret the results better. The Figures 3-5 show sections of the fracture surfaces of the tensile specimens. All fracture surfaces are

perpendicular to the normal stress. No delaminations or detachments of single strands appear. This indicates a good layer bonding. The SEM image in Fig. *3* shows the fracture surface of the specimen with 0.15mm layers.

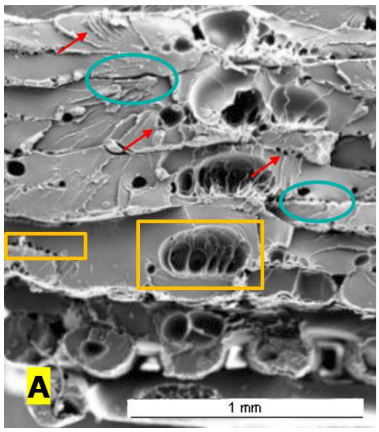

Fig. 3. Fracture surface of 0,15 mm specimen

As with the micrographs, the distinct interlayer pores can be seen. Overall, the inter-layer bonding is insufficient, resulting in inter-layer gaps. The fracture is largely homogeneous but not exclusively in the same plane. The fracture planes change, albeit minimally, across the different layers. Again, this suggests insufficient layer bonding.

In comparison, at 0.1 mm, the number of pores is significantly reduced (Fig. *4*). There are only isolated inter-layer gabs to be found.

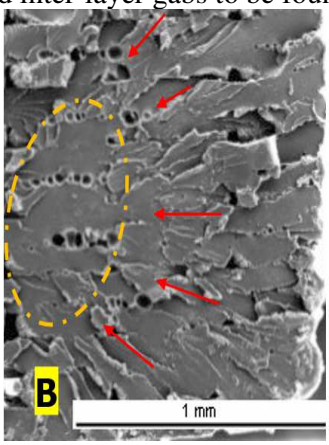

Fig. 4. Fracture surface of 0,1 mm specimen

Nevertheless, the fracture surface in Fig. *4* shows excellent layer bonding. This is evident from the homogeneous and planar fracture surface and the interlayer cracking. The river lines refer to the fracture progression. Starting from a central initial surface, the river lines run almost concentrically, reflecting the crack propagation.

Fig. *5* shows process-related defects. Insufficient material feed and layer overlap resulted in large layer gaps that weakened the structure. As a result, layer bonding to strands in the same plane was not possible or insufficient. In this case, the defect was repeated in the 90° grids. It is striking that the individual strands reflect the largely ductile fracture behavior of the material. The fracture surfaces show significant fracture necking.

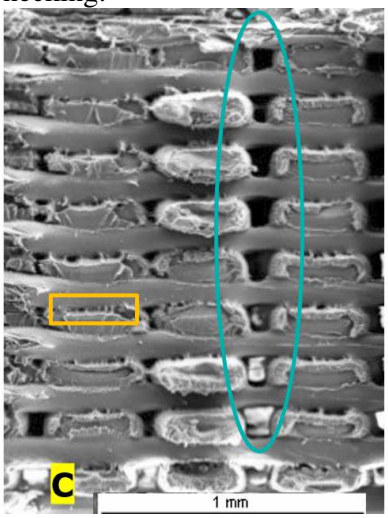

Fig. 5. Fracture surface of 0,1 mm specimen with defects

3.4 Results of the rapid tooling and vulcanization process

It was possible to manufacture a vulcanization mold from PEEK using FFF. The mold printed at room temperature has a partially transparent color due to the FFF process and is in the amorphous state (see Fig. *6*).

After an annealing process the mold became opaque. Also clearly visible is the pronounced stair-step effect created by the layering process. For better adhesion and process reliability, the part was printed on a raft.

Fig. *7* shows the rubber component and a mold half after the successful vulcanization process. It can be seen that the surface of the mold has been copied into the rubber part.

All parts of the mold show no defects or damage. There were also no delaminations that would have revealed an inadequate layer bond. The mold remained dimensionally stable despite a high thermal load of 200°C.

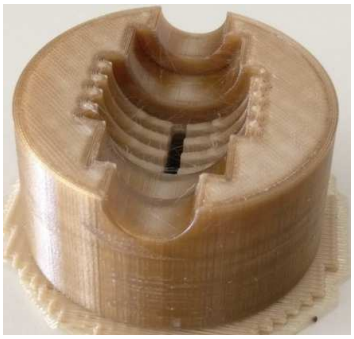

Fig. 6. Mold half – Amorphous state

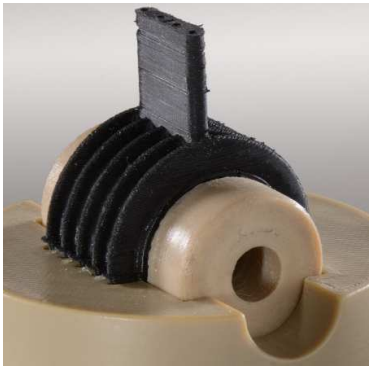

Fig. 7. Annealed PEEK mold and vulcanized rubber component on the mold core

4 CONCLUSIONS

After detailed consideration of the initial process parameters, it is possible to print PEEK at room temperature successfully. The goal is to achieve a high bonding of deposited strands with adjacent strands. This is made possible by a nozzle temperature of at least 410°C and a small layer thickness of 0.1mm. Only with these settings can it be ensured that a spreading neck growth is initiated, and a pore-free print image is achieved. If the temperatures are too low, this leads to the overlapping of different processes. On the one hand, convection leads to rapid cooling of the deposited melt, whose viscosity increases. The high viscosity leads to deformed strands and extreme air entrapment, which cannot leave the melt.

Furthermore, it can be assumed that the interlayer bonding is positively influenced by the heat-affected zone of the nozzle in connection with a minimization of the layer thickness. It should be noted, however, that the AM at room temperature causes the components to solidify amorphously. The low temperatures mean the molecules have no time to reorganize and crystallize. A subsequent annealing process leads to the transformation into the crystalline state. It should be noted here that the components slightly shrink due to the phase transition.

3D printing PEEK at room temperature shows promising results. It has been shown that even at room temperature, a positive effect on tensile strength is achieved by minimizing the layer thickness. At the same time, similar and partly higher tensile strengths were achieved compared to in situ crystallized samples.

Minimizing the layer thickness reduces the pores and improves layer bonding as shown in the micrographs. The defects and pores of the 0.15 mm specimens reduce the tensile area that can absorb the stresses, resulting in local overstresses, as also observed in [28]. Vaezi et al. reports cracking starting in the pores [23]. This is an indicator of pore-induced weak spots. This effect can also be confirmed in the SEM images taken here.

Among others, [10, 25, 29–31] report that BCT $\geq T_g$ lead to higher degree of crystallinity, and improved inter-layer bonding is realized. Thus, the tensile strength can be significantly increased. Yang et al. improved tensile strength from 60 MPa to 85 MPa by increasing BCT from RT to 200°C. However, the study conducted here shows that the post-crystallized samples have similar or slightly higher tensile strength compared to in-situ crystallized samples. The study shows that it is always recommended to thermally post-treat PEEK components.

This study managed the systematic critical comparison of FFF process strategies and the development of a new FFF-PEEK strategy at room temperature. The strategy is based on simplified temperature management that results in amorphously solidifying PEEK components and ensures a stable FFF process.

This approach provides a strategy that facilitates process control and simplifies the equipment technology by eliminating the closed build chamber. The amorphous PEEK components require post-processing thermal treatment for crystallization. With the validated process parameters, the successful qualification and printing of durable PEEK molds for the vulcanization of rubber components at 200°C

was possible. This opens up new possibilities for PEEK in the use of rapid tooling.

5. REFERENCES

[1] Gebhardt, A., Hötter, J.-S., *Additive manufacturing: 3D printing for prototyping and manufacturing,* Hanser Publishers; Hanser Publications, Munich, 2016.

[2] Hubs, *Additive manufacturing technologies poster* | Hubs [Internet], 2023 [modified 2023 Aug 25; cited 2023 Aug 25]. Available from: https://www.hubs.com/get/am-technologies/.

[3] Roland Berger, *Polymer additive manufacturing – Market today and in the future* [Internet], 2020 [modified 2023 Aug 25; cited 2023 Aug 25]. Available from: https://www.rolandberger.com/en/Insights/Publications/Polymer-additive-manufacturing-Market-today-and-in-the-future.html.

[4] Mohamed, O. A., Masood, S. H., Bhowmik, J. L., *Optimization of fused deposition modeling process parameters: a review of current research and future prospects*. Adv. Manuf. 2015, 3, 42–53.

[5] Wang, Y., Müller, W.-D., Rumjahn, A., Schwitalla, A., *Parameters Influencing the Outcome of Additive Manufacturing of Tiny Medical Devices Based on PEEK*. Materials (Basel, Switzerland) 2020, 13.

[6] Cendrero, A. M., Fortunato, G. M., Munoz-Guijosa, et al., *Benefits of Non-Planar Printing Strategies Towards Eco-Efficient* 3D Printing. Sustainability 2021, 13, 1599.

[7] Boparai, K. S., Singh, R., Singh, H., *Development of rapid tooling using fused deposition modeling: a review*. Rapid Prototyping Journal 2016, 22, 281–299.

[8] Rosochowski, A., Matuszak, A., *Rapid tooling: the state of the art.* Journal of Mater Processing Technology 2000, 106, 191–198.

[9] Huzaim, N. H. M., Rahim, S. Z. A., Musa, L., Abdellah, A. E.-H. et al., *Potential of Rapid Tooling in Rapid Heat Cycle Molding: A Review.* Materials 2022, 15.

[10] Zanjanijam, A. R., Major, I., Lyons, J. G., Lafont, U. et al., *Fused Filament Fabrication of PEEK: A Review of Process-Structure-Property Relationships*. Polymers 2020, 12.

[11] Rahman, K. M., Letcher, T., Reese, R., *Mechanical Properties of Additively Manufactured PEEK Components Using Fused Filament Fabrication*, Volume 2A: Advanced Manufacturing. ASME 2015 International Mechanical Engineering Congress and Exposition, Houston, Texas, USA, 13.11.2015 - 19.11.2015, American Society of Mechanical Engineers, 2015.

[12] Ensinger GmbH, *PEEK- Polyetheretherketon: TECAPEEK Kunststoffe von Ensinger* [Internet], 2021 [modified 2021 Nov 9]. Available from: https://www.ensingerplastics.com/de -de/halbzeuge/hochleistungs-kunststoff/peek.

[13] Apium, *Case Study: Mould Making with FFF 3D Printed CFR PEEK Parts - Time and Cost Saving Potential* [Internet], 2019. Available from: https://apiumtec.com/en/case-study-mould-making-with-fff-3d-printed-cfr-peek-parts-time-and-cost-potential.

[14] Dizon, J. R. C., Valino, A. D., Souza, L. R., Espera, A. H. et al., *3D Printed Injection Molds Using Various 3D Printing Technologies.* MSF 2020, 1005, 150–156.

[15] Park, S. J., Lee, J. E., Park, J., Lee, N.-K. et al., *High-temperature 3D printing of polyetheretherketone products: Perspective on industrial manufacturing applications of super engineering plastics*. Materials & Design 2021, 211, 110163.

[16] Vassallo, M., Rochman, A., *Rapid prototyping solution for the production of vulcanized rubber components,* in: p. 150014.

[17] Gao, S., Liu, R., Xin, H., Liang, H. et al., *The Surface Characteristics, Microstructure and Mechanical Properties of PEEK Printed by Fused Deposition Modeling with Different Raster Angles.* Polymers 2021, 14.

[18] Challa, B. T., Gummadi, S. K., Elhattab, K., Ahlstrom, J. et al., *In-house processing of 3D printable polyetheretherketone (PEEK) filaments and the effect of fused deposition modeling parameters on 3D-printed PEEK structures.* The International Journal of Advanced Manufacturing Technology 2022, 121, 1675–1688.

[19] Baek, I., Kwon, O., Lim, C.-M., Park, K. Y. et al., *3D PEEK Objects Fabricated by*

Fused Filament Fabrication (FFF). Materials (Basel, Switzerland) 2022, 15.

[20] Das, A., McIlroy, C., Bortner, M. J., *Advances in modeling transport phenomena in material- extrusion additive manufacturing*. Prog Addit Manuf 2021, 6, 3–17.

[21] Gao, X., Qi, S., Kuang, X., Su, Y. et al., *Fused filament fabrication of polymer materials: A review of interlayer bond*. Additive manufacturing 2021, 37, 101658.

[22] Shahriar, B., et al., *Toward improvement of the properties of parts manufactured by FFF through understanding the influence of temperature and rheological behaviour on the coalescence phenomenon*. Sustainable Technology And Practice For Infrastructure and Community Resilience, Penang, Malaysia, 8–9 August 2017. AIP Conference Proceedings, 2017, p. 40008.

[23] Vaezi, M., Yang, S., *Extrusion-based additive manufacturing of PEEK for biomedical applications.* Virtual and Physical Prototyping 2015, 10, 123–135.

[24] Kumar, R., Singh, G., Chinappan, A., Ghomi, E. R. et al., *On Mechanical, Physical, and Bioactivity Characteristics of Material Extrusion Printed Polyether Ether Ketone*. J. of Mater Eng and Perform 2022.

[25] Wang, R., Cheng, K., Advincula, R. C., Chen, Q., *On the thermal processing and mechanical properties of 3D-printed polyether ether ketone*. MRS Communications 2019, 9, 1046–1052.

[26] Zhang, J., et al., *T4F3: temperature for fused filament fabrication.* Prog Addit Manuf 2022, 7, 971–991.

[27] Herwig, H., Moschallski, A., *Wärmeübertragung,* Springer Fachmedien Wiesbaden, Wiesbaden 2019.

[28] Li, Q., Zhao, W., Li, Y., Yang, W. et al., *Flexural Properties and Fracture Behavior of CF/PEEK in Orthogonal Building Orientation by FDM: Microstructure and Mechanism.* Polymers 2019, 11.

[29] Yang, C., Tian, X., Li, D., Cao, Y. et al., *Influence of thermal processing conditions in 3D printing on the crystallinity and mechanical properties of PEEK material.* J of Mat ProcTechnology 2017, 248, 1–7.

[30] Yang, D., Cao, Y., Zhang, Z., Yin, Y. et al., *Effects of crystallinity control on mechanical properties of 3D-printed short-carbon-fiber-reinforced polyether ether ketone composites*. Polymer Testing 2021, 97, 107149.

[31] Vanaei, H. R., Shirinbayan, M., Deligant, M., Khelladi, S. et al., *In-Process Monitoring of Temperature Evolution during Fused Filament Fabrication: A Journey from Numerical to Experimental Approaches*. Thermo 2021, 1, 332–360.

POLIETERETERCETONA (PEEK) ÎN RAPID TOOLING: PROGRESE ȘI APLICAȚII PENTRU FFF A MATRIȚELOR DIN CAUCIUC

Rezumat: Introducerea polimerilor de înaltă performanță în fabricarea aditivă deschide noi aplicații industriale. Polieteretercetona (PEEK) a fost utilizată inițial în industria aerospațială, dar in prezent este aplicată pe scară largă în industria auto, electronică și medicală. Acest studiu se concentrează pe dezvoltarea de aplicații care utilizează PEEK și fabricarea prin depunere de material topit pentru producția de matrițe de injecție din cauciuc, rentabile și eficiente din punct de vedere al costurilor. Un stuiu al conceptului confirmă că PEEK este potrivit pentru fabricarea de matrițe prin AM, rezistentă la condițiile de utilizare. Imprimarea PEEK peste temperatura sa de tranziție vitroasă de 145 °C este preferabilă datorită intervalului restrans de procesare. Se discută o nouă strategie de procesare la temperatura ambientala, cu micrografii care arată o legătură între straturi îmbunătățită la o temperatură a duzei de 410 °C și o grosime a stratului de 0,1 mm. Minimizarea grosimii stratului de la 0,15 mm la 0,1 mm îmbunătățește rezistența la tracțiune cu 16%.

Karim ABBAS, PhD Std., Eng., University of Applied Sciences Aachen, Faculty of Mechanical Engineering and Mechatronics, Goethestr. 1, 52064 Aachen, Germany, abbas@fh-aachen.de .

Nicolae BALC, Prof.dr.eng., Technical University of Cluj-Napoca, Department of Manufacturing Engineering, Bdul Muncii,103-105, 400641 Cluj-Napoca, Romania, nicolae.balc@tcm.utcluj.ro

Sebastian BREMEN, Prof.dr.eng., bremen@fh-aachen.de .

Lukas HEDWIG, University of Applied Sciences Aachen, Faculty of Mechanical Engineering and Mechatronics, Goethestr. 1, 52064 Aachen, Germany